



Numerical Investigation on the Head-on Quenching (HoQ) of Laminar Premixed Lean to Stoichiometric Ammonia–Hydrogen–Air Flames

Chunkan Yu¹ · Liming Cai² · Cheng Chi³ · Syed Mashruk⁴ · Agustin Valera-Medina⁴ · Ulrich Maas¹

Received: 27 April 2023 / Accepted: 6 September 2023
© The Author(s) 2023

Abstract

The Head-on Quenching (HoQ) of laminar premixed ammonia–hydrogen–air flames under lean to stoichiometric condition is numerical investigated. Detailed chemistry including 34 reactive species and detailed multi-component transport model including thermal diffusion (Soret effect) are applied. The quenching distance is considered as a representative quantity for the HoQ process, and the influence of different system parameters on it has been investigated. These parameters involve fuel/air equivalence ratios, hydrogen content in gas mixture and pressure. It was found that an increase of quenching distance can be caused by a lower hydrogen addition and a leaner mixture condition. Furthermore, it was found that, regardless of the gas mixture, the quenching distance decreases monotonically with increasing pressure, obeying a power function with the exponent -0.7 . Moreover, numerical results show a relation between the quenching Peclet number and the dimensionless wall heat flux normalized by the flame power. Additionally, sensitivities of quenching distances with respect to the transport model, considering the heat loss in the wall and the chemical kinetics are studied.

Keywords Ammonia–hydrogen · Premixed flame · Head-on quenching · Sensitivity analysis · Chemical kinetics

✉ Chunkan Yu
chunkan.yu@kit.edu

¹ Institute of Technical Thermodynamics, Karlsruhe Institute of Technology, Engelbert-Arnold-Straße 4, 76131 Karlsruhe, Baden-Württemberg, Germany

² School of Automotive Studies, Tongji University, Cao'an Road No.4800, Shanghai 201804, People's Republic of China

³ Laboratory of Fluid Dynamics and Technical Flows, Otto-von-Guericke-Universität Magdeburg, Universitaetsplatz 2, 39106 Magdeburg, Sachsen-Anhalt, Germany

⁴ College of Physical Sciences and Engineering, Cardiff University, C4.05, Queen's Buildings - Central Building, 5 The Parade, Newport Road, Cardiff CF24 3AA, UK

1 Introduction

In most engineering applications such as gas turbines and internal combustion engines, flame quenching due to flame-wall interaction (FWI) is an important topic, since it involves numerous physico-chemical processes such as formation of pollutants or the flame stability (Potter Jr 1960; Daniel 1957; Ferguson and Keck 1977; Bruneaux et al. 1996; Lai et al. 2018; Salimath et al. 2020). Due to its importance, the flame-wall interaction has been intensively studied from numerical or experimental aspects for different configurations of FWI (Poinsot and Veynante 2005), namely the (i) Head-on Quenching (HoQ), where the flame propagates towards the wall and the flame front is parallel to the wall; (ii) Side-Wall Quenching (SWQ), where the flame front is perpendicular to the wall; and (iii) tube quenching, where the flame propagates inside the tubes and can quench in case of tubes with sufficient small diameter. In the last decades, the FWI investigation has been performed for various fuels such as hydrogen (Gruber et al. 2010; Mari et al. 2016; Yenerdag et al. 2017), hydrocarbon (Häber and Suntutz 2018; Andrae et al. 2002; Popp et al. 1996; Baigmohammadi et al. 2020; Kosaka et al. 2020) and Biofuels (Kosaka et al. 2020; Kaddar et al. 2022; Wan et al. 2019).

Ammonia (NH_3) has been considered as next generation fuel because it can be produced by using renewable energy sources such as solar and wind energy (Valera-Medina et al. 2018, 2021), with which the goal of net zero-carbon emission can be achieved. While the combustion processes of ammonia-based fuels such as auto-ignition (Li et al. 2019; He et al. 2019; Dai et al. 2020) and flame propagation (Mei et al. 2019; da Rocha et al. 2019; Jing et al. 2021; Chi et al. 2022) have been intensively studied in recent years, limited literature involving its interaction with solid wall, to author's knowledge, can be found. In Okafor et al. (2021) the influence of wall heat loss on the premixed ammonia-air swirling flames interacting with the combustor wall has been experimental studied by employing Planar Laser-Induced Fluorescence (PLIF) imaging of OH radicals and Fourier Transform Infrared (FTIR) spectrometry, and it is found that large heat loss in the wall results in the flame quenching and large amount of unburnt NH_3 emission. In Wei et al. (2021) the stabilization characteristics of NH_3 -air premixed flame near blow-off limit of NH_3 /air flame numerical studied using the Large Eddy Simulation (LES), and it is found that the wall heat loss showed greater influence on NH_3 -air flame stabilization. In Yu et al. (2023) the steady laminar stagnation flow NH_3 - H_2 -air premixed flame was considered and the thermal stresses in the plane wall induced by the combustion processes have been investigated, and it is found that the solid wall would probably undergo plastical deformation under certain conditions such as high strain rates (corresponding to high flow velocity) and high pressures. Furthermore, the larger the heat conductivity of the wall has, the more stable is the flame against extinction.

Our objective in this work is to explore the flame-wall interaction of unstrained premixed NH_3 - H_2 -air flames and the quenching behavior, which is, to author's knowledge, less investigated. The Head-on Quenching (HoQ) process will be considered, because this is a nice canonical configuration which can be described by only one spatial coordinate, and the corresponding governing equations for mass, species, momentum and energy can be simplified to one-dimensional formulation. Furthermore, the numerical simulation can be performed by using detailed transport models and detailed chemical kinetics, without increasing the computational cost significantly. Nevertheless, the flow patterns in real combustion applications are very complex and some phenomenon such as shear flow effect and preferential diffusion effect in different directions may add additional effect on the flame,

but such a model is beyond the scope of this paper. This work aims at studying the idealized one-dimensional laminar flame model, and give the first insight into the HoQ process of the ammonia system.

In the present work, the focus will be on the hydrogen-enriched ammonia-air mixture, because the addition of hydrogen can improve the combustion efficiency and stability to overcome the low reactivity and easy distinguish of pure ammonia-air system (Valera-Medina et al. 2021, 2018). Furthermore, we will focus on the lean to stoichiometric combustion. Such combustion is of great interesting, because various groups are now considering the use of ammonia for replacement in current gas turbines which operate under Dry Low NOx (DLN) conditions that fall into the lean regime with single-stage combustion chambers. Khateeb et al. (2021) conducted the first studies showing that ammonia could be burned under lean conditions close to operational gas turbine equivalence ratios. The results showed that NO tends to decrease with equivalence ratio, whilst stability was somehow degraded. The work opened further research for high-pressure analyses of these lean ammonia/hydrogen blends (Khateeb 2020). However, further analyses performed by Mashruk et al. (2022) showed that those conditions of operation would be detrimental to the production of N_2O , as the heat losses of these lean flames promote reactions such as $NO + NH \rightarrow N_2O + H$ at the flame front, hence generating this powerful greenhouse gas (i.e. 300 times more damaging than CO_2). Nevertheless, the potential of using lean combustion conditions to ensure minor retrofitting of current gas turbine units is economically attractive, thus requiring further research to decrease heat losses whilst understanding the reaction mechanisms behind the interaction of radicals such as NH (mainly produced via OH pools) under these conditions.

The main result parts will be divided into two parts:

- In the first part, the quenching distance will be discussed. The influence of the system parameters such as the mixture compositions (incl. equivalent ratios and hydrogen content) and the system pressures on the quenching distance will be investigated.
- In the second part, the results will focus on the influence of different numerical models such as the molecular transport models, considering the heat loss in the wall and reaction mechanisms. It will be discussed how the predicted quenching distances vary with different numerical models.

2 Mathematical Modeling

2.1 Numerical Method and Model Configuration

To study the FWI numerically, the in-house code *INSFLA* (Maas and Warnatz 1988) has been used. This code solves for the spatio-temporal evolution of the system of PDEs for the given initial and boundary conditions using the method of lines. *INSFLA* has the advantage that a non-uniform grid is used and is automatically adapted according to the instantaneous flame structure. Furthermore, it involves an automatic adaptive time stepping with order and stepsize control, such that significant computational time can be saved without losing accuracy. The code *INSFLA* has already been validated for the FWI including differential diffusion and surface reactions for different combustion systems such as methane/air and iso-octane/air mixtures (Strassacker et al. 2018, 2019, 2021).

In the numerical calculation, a detailed molecular transport model, the multi-component diffusion model including the thermal diffusion (Soret effect: molecular diffusion due to temperature gradient), is applied. The multi-component diffusion model takes into account the differential diffusion caused by different species, and the diffusion coefficient of each species into the mixture depends on the instantaneous mixture composition. The formulation for the diffusion fluxes $j_{i,g}$ is written as Hirschfelder et al. (1964):

$$j_i = j_i^M + j_i^T = -\rho D_i^M \frac{w_i}{x_i} \frac{\partial x_i}{\partial z} - \frac{D_i^T}{T} \frac{\partial T}{\partial z}, \quad (1)$$

where x_i is the mole fraction of i -th species. D_i^M represents the mixture-averaged diffusion coefficient, and D_i^T the thermal diffusion coefficient for the Soret effect. Both D_i^M and D_i^T are calculated according to Ref. Hirschfelder et al. (1964). Note that more detailed models such as Maxwell-Stefan model (Bothe 2011) are available, but it has been shown that the multi-component diffusion model and the mixture-averaged diffusion model give similar prediction for the flame quenching at a cold wall (Ganter et al. 2017; Zirwes et al. 2021). Moreover, according to Popp and Baum (1997), the Dufour effect for the head-on quenching is negligible.

Furthermore, the thermal conductivity of gas mixture is calculated via

$$\lambda = 0.5 \left(\sum_i^{n_s} x_i \lambda_i + \frac{1}{\sum_i^{n_s} \frac{x_i}{\lambda_i}} \right), \quad (2)$$

where λ_i is the heat conductivity of i -th species determined by the Chapman-Enskog solution of kinetic gas theory (Kee et al. 2005).

The Head-on Quenching (HoQ) configuration studied in the present work is illustrated in Fig. 1. The laminar flat flame, which is considered as initial condition, is propagating to a cold wall and quenches there due to heat loss to the cold wall. The wall is located at $x = 0$ m, and the unburnt gas (cold premixed gas) has the same temperature as the cold wall temperature: $T_{ub} = T_w = 300$ K. Since the wall temperature is sufficiently low, the impact of the surface reactions is negligible small and the wall can be approximately considered as inert here Popp and Baum (1997). For this reason, the boundary condition for the species diffusion flux $j_{i,x}$ at the wall can be formulated as

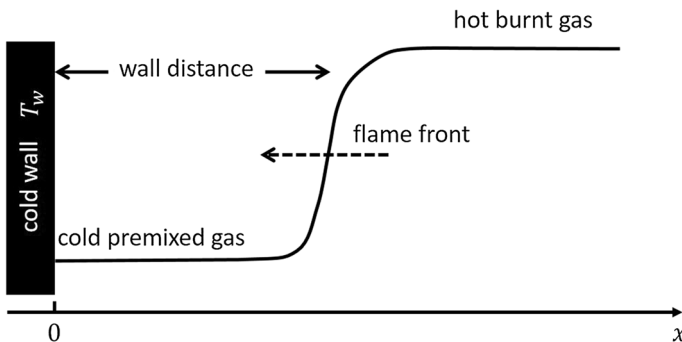


Fig. 1 Schematic illustration of Head-on Quenching (HoQ)

$$j_{i,x}(x = 0^+) = j_{i,x}^M(x = 0^+) + j_{i,x}^T(x = 0^+) = 0, \quad (3)$$

where $j_{i,x}^M$ is the mass diffusion determined by the Fick's law and $j_{i,x}^T$ the thermal diffusion describing the Soret effect (Hirschfelder et al. 1964)

At the right domain, there exists hot burnt gas and the gradient of temperature T and mass fractions of all species w_i are set to be zero:

$$\frac{\partial T}{\partial x}(x = \Omega) = \frac{\partial w_i}{\partial x}(x = \Omega) = 0, \quad (4)$$

where Ω is the length of the whole computational domain.

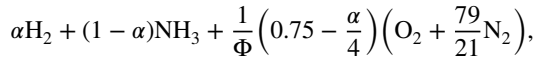
Moreover, the pressure p is considered to be constant.

In Table 1 we list all the relevant boundary and initial conditions applied in our numerical simulation, as described in this section.

2.2 Combustion System

2.2.1 Gas Mixture

In this work, the H_2 -enriched ammonia-air (NH_3 - H_2 -air) mixtures are considered. The addition of H_2 in the gas mixtures is described by the mole fraction α of H_2 in the fuel:



where Φ is the fuel/air equivalence ratio. For $\alpha = 0$ we have pure ammonia-air mixture, and for $\alpha = 1$ pure hydrogen-air mixture. Although the HoQ behavior of the NH_3 - H_2 -air mixture is the focus of this work, pure NH_3 -air mixture and pure H_2 -air mixture are also considered as references to compare the performance.

For the mixture compositions, we focus on varying H_2 content with $0 \leq \alpha \leq 0.4$, as such level of H_2 addition keeps ammonia-based features whilst being more representative to future industrial systems working on NH_3 - H_2 blends (Valera-Medina et al. 2018, 2021).

Furthermore, the fuel/air equivalence ratios are selected to be $0.6 \leq \Phi \leq 1.0$. Since, as mentioned in the introduction section, various groups are now considering the use of ammonia for replacement in current gas turbines which operate under Dry Low NOx (DLN) conditions that fall into the lean regime with single-stage combustion chambers.

2.2.2 Effective Lewis Number of Unburnt Gas Mixture

A very important property of ammonia with different levels of hydrogen additions is the significant differences on molecular transport, because hydrogen is much lighter than ammonia and thus a faster diffusion. Therefore, it is helpful to check the Lewis number of gas mixture Le_{eff} . Note that there are various ways to determine the Le_{eff} such as volume-based, diffusion-based and heat-release based formulation. However we are not focusing on investigating the correctness of various formulations in this work, but on using it to check the differential diffusion effect caused by hydrogen addition, we use the simplest way, the volume-based formulation, to calculate the Le_{eff} . Some reviews and comparison of different formulations can be

Table 1 Boundary conditions for the numerical simulation

Boundary conditions	
Left boundary $x = 0^+$	$T_{\text{ub}} = T_w = 300 \text{ K}$ $J_{i,x} = 0$ (c.f. Eq. 3) $w_i = w_{i,\text{ub}}$ p
right boundary $x = \Omega$	Temperature Species diffusion flux Species mass fraction Pressure Species mass fraction Temperature Pressure
Initial condition for $t = 0$	$\frac{\partial w_i}{\partial x} = 0$ $\frac{\partial T}{\partial x} = 0$ p
Unstrained premixed flame under adiabatic condition	

found in e.g. Bouvet et al. (2013), Lapalme et al. (2017), Savard and Blanquart (2014), Hou et al. (2022). The volume-based formulation for Le_{eff} consists of two steps:

- Calculate the Lewis number Le_{NH_3} and Le_{H_2} of species NH_3 and H_2 via

$$Le_i = \frac{a_{\text{ub}}^{\text{mix}}}{D_{i,\text{ub}}} = \frac{\lambda_{\text{ub}}^{\text{mix}}}{\rho_{\text{ub}}^{\text{mix}} \cdot c_{p,\text{ub}}^{\text{mix}} \cdot D_{i,\text{ub}}}, \tag{5}$$

where $a_{\text{ub}}^{\text{mix}}$, $\lambda_{\text{ub}}^{\text{mix}}$, $\rho_{\text{ub}}^{\text{mix}}$ and $c_{p,\text{ub}}^{\text{mix}}$ are the thermal diffusivity, heat conductivity, density and isobaric specific heat capacity of unburnt $\text{NH}_3\text{-H}_2\text{-air}$ gas mixture. $D_{i,\text{ub}}$ is the molecular diffusivity of species i in unburnt gas mixture.

- Calculate the Le_{eff} based on the mole fractions in fuel via (Ichikawa et al. 2015)

$$Le_{\text{eff}} = \frac{x_{\text{NH}_3} + x_{\text{H}_2} + x_{\text{O}_2}}{\frac{x_{\text{NH}_3}}{Le_{\text{NH}_3}} + \frac{x_{\text{H}_2}}{Le_{\text{H}_2}} + \frac{x_{\text{O}_2}}{Le_{\text{O}_2}}}. \tag{6}$$

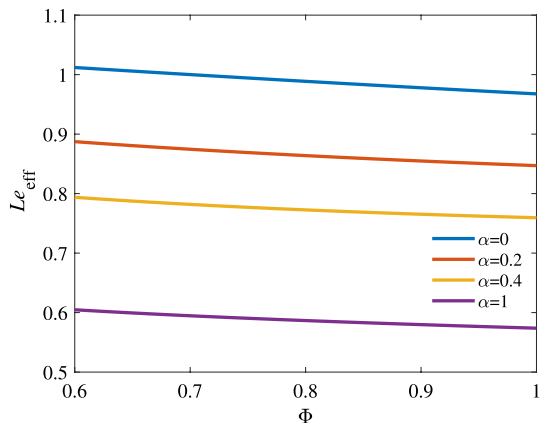
Figure 2 compares the Lewis number of fuel Le_{eff} of gas mixture with different levels of hydrogen addition for fuel/air equivalence ratios Φ at $T_{\text{ub}} = 300 \text{ K}$ and $p = 1 \text{ bar}$. We observe that the effect of hydrogen addition in gas mixture on the Le_{eff} is much more significant than of the fuel/air equivalence ratios Φ . The more the hydrogen is added into gas mixture, the smaller is the Le_{eff} .

2.2.3 Flame Thickness of the Unstrained Premixed Flame

Later, the quenching Peclet number will be introduced where the quenching distance is normalized by the flame thickness (see below). Therefore, the flame thickness for the considered combustion system will be shortly discussed. According to Bychkov and Liberman (2000) the flame thickness δ_f can be evaluated using the dimensional analysis

$$\delta_f = \frac{a_{\text{ub}}}{s_f}, \tag{7}$$

Fig. 2 effective Lewis number Le_{eff} versus fuel/air equivalence ratios Φ for gas mixture with different hydrogen addition at $T_{\text{ub}} = 300 \text{ K}$ and $p = 1 \text{ bar}$



where a_{ub} is the thermal diffusivity of the unburnt premixed gas mixture, and s_f the laminar flame speed of unstrained premixed flame. Note that although there are also many other definitions for the flame thickness such as the thermal flame thickness estimated by considering the temperature gradient ($\delta_f = (T_b - T_{ub}) / (dT/dx)_{max}$), they will not be considered here because the tendency of flame thickness depending on the fuel/air equivalent ratio Φ and the hydrogen content α does not alter by considering other definition for flame thickness.

In Fig. 3 the flame thickness δ_f is plotted against fuel/air equivalence ratios Φ for gas mixtures with different hydrogen addition at $T_{ub} = 300$ K and $p = 1$ bar. It is observed that the flame thickness decreases with increasing hydrogen content and fuel/air equivalent ratios in regime $0.6 \leq \Phi \leq 1.0$, which is also confirmed in e.g. Li et al. (2014).

2.3 Chemical Mechanism

For the numerical simulation, the Li-2019 detailed chemical mechanism is applied (Li et al. 2019). This mechanism is originally designed for $NH_3-H_2-CH_4$ air combustion system, which has been intensively validated and documented for the ignition delay times (IDT), laminar burning velocities (LBV), and speciation (Li et al. 2019). To avoid unnecessary computational cost for inert gas such as Ar and He and carbon-related species, these species are removed and the remaining mechanism has 34 species and 252 reactions.

3 Quenching Process and Quenching Distance

Figure 4 shows one representative quenching process. In the first phase, the flame propagates towards the wall. Since the flame is still far from the wall, the cold wall has no influence on the flame structure (here black and purple solid lines). During the second stage, flame approaches the wall and the cold wall begins to affect the flame structure. The closer the flame approaches the wall, the larger is the heat loss towards the wall. When the heat loss becomes sufficiently large, the heat release inside the flame is not large enough to support the flame propagation and thus flame starts to quench.

According to the Fourier's law, the heat loss to the cold wall \dot{q}_w can be calculated as:

Fig. 3 Flame thickness δ_f versus fuel/air equivalence ratios Φ for gas mixture with different hydrogen addition at $T_{ub} = 300$ K and $p = 1$ bar

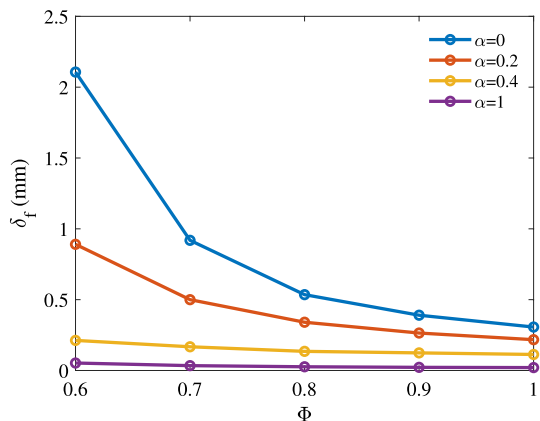
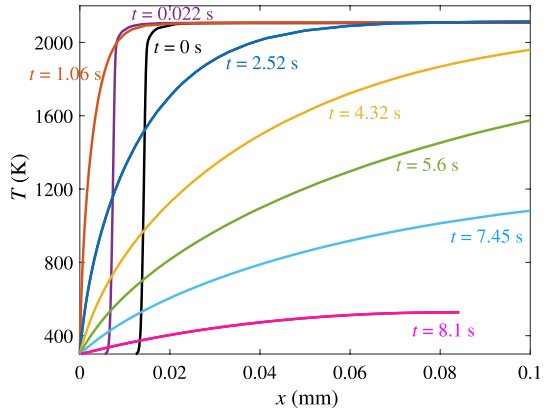


Fig. 4 Representative quenching process. Temperature profile for different times



$$\dot{q}_w = -\lambda(x = 0^+) \cdot \left. \frac{\partial T}{\partial x} \right|_{x=0^+}, \tag{8}$$

where λ is the heat conductivity of gas mixture. The flame quenches, after the heat loss \dot{q}_w has reached its maximum. And the corresponding quenching distance d_q is the distance between the cold wall and the location of the maximum of the total heat release rate (HRR), which is defined as:

$$\text{HRR} = \sum_{i=1}^{n_s} \dot{\omega}_i h_i, \tag{9}$$

where $\dot{\omega}_i$ and h_i are the net production rate and enthalpy for species i .

Figure 5 shows representative temperature (T), heat release rate (HRR) and species mole fractions profiles at the time of quenching. It is interesting to mention that the left figure shows non-zero HRR at the wall ($x = 0$), which is consistent with the observation in Dabireau et al. (2003), Palulli et al. (2019), Owston et al. (2007). As discussed there, such non-zero HRR at the wall is attributed to the low-temperature induced radical recombination reactions, which can contribute over 50% to the total HRR at the wall.

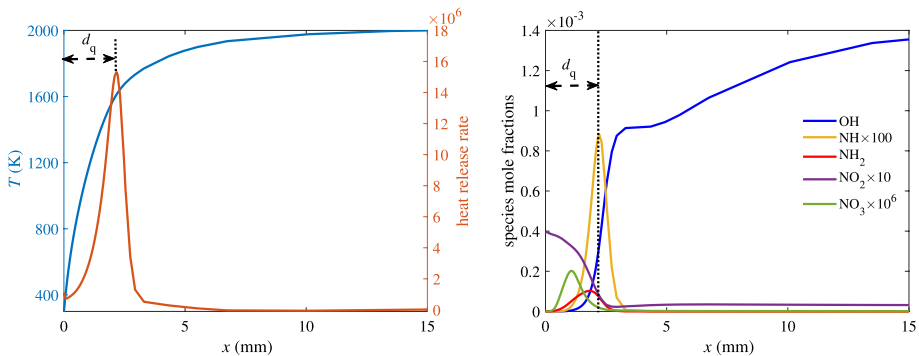


Fig. 5 Example of temperature (T), heat release rate (HRR) and species mass fractions profiles over spatial coordinate at quenching time

Furthermore, as studied in Poinso et al. (1993), Vosen et al. (1985), Boust et al. (2007), Bruneaux et al. (1996) by means of the analytical solution for the HoQ premixed flames, two important dimensionless quantities can be introduced, which are helpful for the analysis of quenching processes for different fuel types and are correlated with each other. They are the quenching Peclet number Pe_q and the normalized wall heat loss φ :

- The quenching Peclet number is defined as

$$Pe_q = \frac{d_q}{\delta_f}, \quad (10)$$

where d_q is the quenching distance and δ_f is the flame thickness (c.f. Eq. 7). Various works (Poinso et al. 1993; Boust et al. 2007; Popp and Baum 1997; Chauvy et al. 2010; Guiberti et al. 2020) have already confirmed both numerical and experimental, that the quenching Peclet number Pe_q is in the order of three ($Pe_q \approx 3.0$) for methane-air flames. However, this quenching Peclet number varies noticeable with fuel types. In Rißmann et al. (2017) they showed that for C_2H_4 $Pe_q \approx 5.5$, and $Pe_q \approx 1.4$ or 1.7 for H_2 flame (Dabireau et al. 2003; Gruber et al. 2010). Moreover, in Lai and Chakraborty (2016) it is stated based on the DNS analysis that smaller Lewis numbers could lead to higher quenching Peclet numbers.

- The normalized wall heat loss φ is defined as

$$\varphi = \frac{\max(\dot{q}_w)}{Q_\Sigma}, \quad (11)$$

describing the wall heat loss at the quenching moment $\max(\dot{q}_w)$ normalized by the so-called “flame power” Q_Σ which can be determined as Boust et al. (2007), Poinso et al. (1993), Bruneaux et al. (1996)

$$Q_\Sigma = \rho_{ub} c_p s_f (T_b - T_{ub}) \quad (12)$$

The analytical thermal formulation for quenching of transient laminar flames at cold wall in Boust et al. (2007) shows that φ and Pe_q are correlated in a simple relation approximately as:

$$\varphi = \frac{1}{Pe_q + 1}. \quad (13)$$

More details can be found in Boust et al. (2007). One must, however, emphasize at this stage that this simple relation is based on the pure thermal transport analysis, and the influence of species transport on the quenching processes is not considered in this analytical thermal formulation. Later we will investigate the relation between both quantities for NH_3 - H_2 -air system.

4 Results: Phenomenology Discussion on Quenching Distance

In this section, we will focus on the effect of three different system parameters on the quenching distance d_q , namely the fuel/air equivalence ratio $0.6 \leq \Phi \leq 1.0$, the pressure $1 \text{ bar} \leq p \leq 20 \text{ bar}$ and the hydrogen addition in the mixture $0 \leq \alpha \leq 0.4$. Figure 6 shows

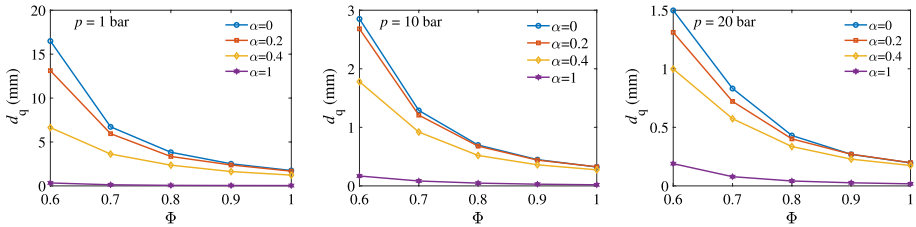


Fig. 6 Quenching distance d_q (mm) over fuel/air equivalence ratios Φ for different hydrogen additions and different pressures

the dependence of d_q on these three system parameters, which will be discussed in the following.

4.1 Influence of Mixture Composition

As shown in Fig. 6, for all pressures and fuel/air equivalence ratios, the quenching distances d_q decreases with increasing hydrogen content in the gas mixture monotonically. According to the numerical simulation involving total heat release rate at various hydrogen addition in Li et al. (2019), the more hydrogen added in the mixture, the higher heat release rate has the mixture. Therefore, flames of mixture with higher hydrogen contents are capable of losing more heat to the cold wall. In this sense, the higher the hydrogen added into the mixture, the closer the flame reaches the cold wall and remains stable against quenching. This effect of hydrogen addition in the ammonia system is also consistent with the behavior in methane-hydrogen systems (Guo et al. 2022).

Moreover, Fig. 6 further shows that the quenching distances d_q decreases with increasing fuel/air equivalence ratios monotonically in range of lean to stoichiometric conditions for all pressures, which is also consistent to the analysis that the flame speed reaches its maximum in the stoichiometric condition and thus the d_q its minimum.

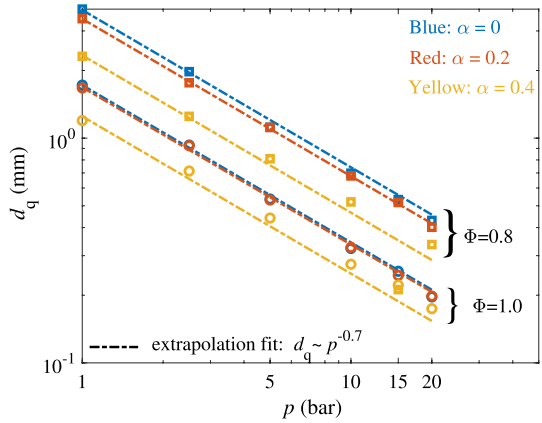
4.2 Influence of Pressure

In the following, the influence of pressure on the quenching distance will be discussed, as shown in Fig. 7 where different fuel/air equivalence ratios and hydrogen addition in mixtures are considered. To clarify the pressure-dependence, a least-square extrapolation fit of a power function $d_q \sim p^a$ is also included, which is also used in e.g. Refs. Suckart et al. (2017), Boust et al. (2007).

It is mainly observed here that the quenching distance decreases monotonically with increasing pressures for all cases. Such dependence has also been confirmed by experimental and analytical investigation in other literature focusing on methane-air flame with $d_q \sim p^{-0.56}$ (Westbrook et al. 1981), gasoline flame with $d_q \sim p^{-0.55}$ (Suckart et al. 2017) and methanol flame with $d_q \sim p^{-0.88}$ (Westbrook et al. 1981). This trend is attributed to the fact, as discussed in Refs. Chu et al. (2019), Boust et al. (2007), Colson et al. (2016), Westbrook et al. (1981), that a higher pressure increases the chemical reaction rate in terms of higher collision rate of reactive molecules, resulting in a growth of heat release rate (HRR). Thus, flame can get closer to the wall and more resistant to quenching.

Based on the numerical prediction, the correlation between quenching distance d_q and pressure p by using the power function reads:

Fig. 7 Quenching distances versus pressure for gas mixture with different hydrogen addition and fuel/air equivalence ratios $\Phi = 0.8$ and $\Phi = 1.0$. Both axes in logarithmic scales



$$d_q \sim p^{-0.7}. \tag{14}$$

In Zhang et al. (2022), it is suggested that the laminar flame speed of ammonia–hydrogen–air system S_u also follows a power function of pressure as $S_u \sim p^{-0.32}$. Therefore a correlation between $d_q \cdot S_u$ and the pressure has the form

$$d_q \cdot S_u \sim p^{-0.7} \cdot p^{-0.32} = p^{-1.02}, \tag{15}$$

which is consistent with the correlation form of $d_q \cdot S_u \sim p^{-1.0}$ for both methane- and methanol-air system as shown by Westbrook et al. (1981).

4.3 Quenching Peclet Number Pe_q and Normalized Wall Heat Loss φ

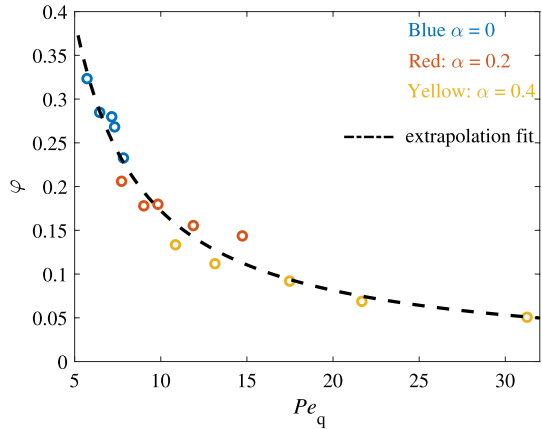
As mentioned above, the Quenching Peclet number Pe_q normalized wall heat loss φ are two important quantities in the description of the transient quenching processes, which takes into account different gas mixtures, and a simple relation is proposed based on thermal transport analysis. In this part, the relation between quenching Peclet number and the normalized wall heat loss introduced in Sect. 3 for gas mixtures with different hydrogen additions are presented in Fig. 8. The aim of this part is to investigate whether a similar simple relation is also valid for ammonia–hydrogen systems with different hydrogen contents.

We observe from Fig. 8 clearly that the quenching Peclet numbers Pe_q vary significantly for different gas mixtures, and are different from those of the hydrocarbon system with values around 3.0–5.5 (Poinsot et al. 1993; Boust et al. 2007; Popp and Baum 1997; Chauvy et al. 2010; Guiberti et al. 2020; Rißmann et al. 2017; Ganter et al. 2017). However, a similar relation proposed in Boust et al. (2007) can be observed, namely an increase of Pe_q leads to decreasing normalized wall heat loss φ and vice versa. Furthermore, an empirical extrapolation fit shows a correlation

$$\varphi = \frac{1.54}{Pe_q - 1.07}, \tag{16}$$

which is close to the theoretical formulation derived in Boust et al. (2007) (c.f. Eq. 13). However, it should be emphasized here that the simple relation proposed in Boust et al. (2007) is only based on the thermal transport analysis, and the complexity of molecular

Fig. 8 Relation between quenching Peclet number Pe_q and normalized wall heat loss φ for gas mixture with different hydrogen additions under $p = 1$ bar



diffusion transport is not taken into account, which leads to a difference in the correlation between φ and Pe_q .

However, this result shows that the usage of normalized wall heat loss φ is helpful for the study of quenching process for the $\text{NH}_3\text{-H}_2\text{-air}$ combustion system, since they include the influence of different gas mixtures on the combustion properties in terms of e.g. the fuel mass fraction, enthalpy of reaction and laminar flame speeds.

5 Results: Sensitivity of the Simulated Quenching Distance

Due to the lack of experimental measurement, the discussion above is rather quantitative. In this results section, we focus on to check which physical and chemical models are important in the prediction of quenching distances.

5.1 Transport Model

All the results in Sect. 4 were calculated using the detailed multi-component transport model including the thermal diffusion. In this part, it is interesting to see whether the transport model could have impact on the quenching distances. In order to answer this question, we use other two different transport models: (1) multi-component transport model without thermal diffusion; (2) unity Lewis number model (equal diffusivity for all species).

In the unity Lewis number model, all the species have the same diffusion coefficient which is computed as:

$$D = D_i = \frac{\lambda}{\rho c_p}, \quad (17)$$

where λ , ρ and c_p are the heat conductivity, density and isobaric heat capacity of the gas mixture. It should be mentioned here that the heat conductivity and viscosity of the gas mixture are still computed in a detailed way without any simplification.

Figure 9 shows two representative results of predicted quenching distances over fuel/air equivalence ratios by using different diffusion models for pure $\text{NH}_3\text{-air}$ flames ($\alpha = 0$) and $\text{NH}_3\text{-H}_2\text{-air}$ flames with 20 and 40% hydrogen addition ($\alpha = 0.2$ and

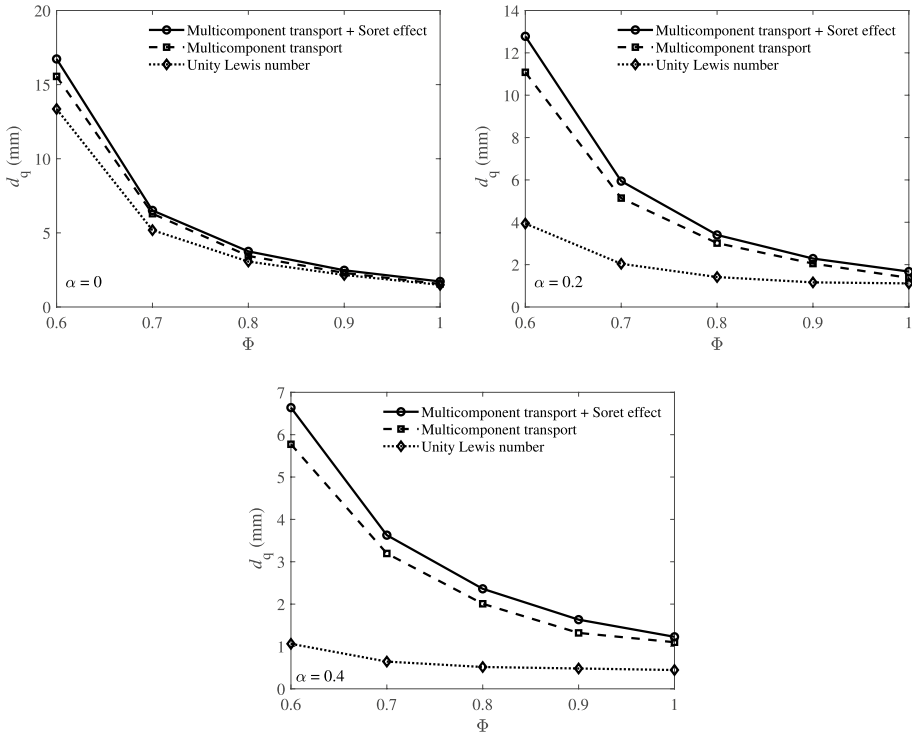


Fig. 9 Quenching distances versus fuel/air equivalence ratio for gas mixture with $\alpha = 0, 0.2$ and 0.4 at $p = 1$ bar using different diffusion models

$\alpha = 0.4$). It is observed that the predicted quenching distances are more significantly affected by the diffusion models with increasing hydrogen contents, which is also expected. For pure NH_3 -air flames whose effective Lewis number of fuel is around unity ($Le_{\text{eff}} \approx 1$, c.f. Fig. 2), the deviation between using very detailed transport model (circle solid lines) and using the unity Lewis number model (diamond point lines) is maximum around 20% at $\Phi = 0.6$. However, for NH_3 - H_2 -air flames with 20% hydrogen addition ($\alpha = 0.2$), the use of unity Lewis number model predicts almost 3 times smaller compared to those using very detailed transport model (multicomponent transport + Soret effect), and the discrepancy increases further if the hydrogen content is further increased (almost 7 times smaller for $\Phi = 0.6$). The large difference caused by using the unity Lewis number model has also been confirmed in the hydrocarbon-air system such as shown in Zirwes et al. (2021); Ganter et al. (2017).

The Soret effect, on the other hand, plays a smaller role in the prediction of the quenching distance, compared to those predicted by the unity lewis diffusion model. This is also consistent with Popp and Baum (1997). However, it should be mentioned that the Soret effect can still alter the prediction of quenching distance, because as discussed in Kovaleva et al. (2023) the Soret effect accelerates the diffusion of H_2 towards the flame front and shifts the position of the temperature profile towards the lean conditions. This is also consistent with the observation in Wang et al. (2021), Liang et al.

(2013) that the Soret effect becomes especially important for hydrogen and high hydrogen contained combustion system.

5.2 Conjugate Heat Loss in the Wall

Till now, all the calculations above are based on the assumption that the wall temperature at $x = 0$ in Fig. 1 was fixed. In this subsection, the mathematical model introduced in Sect. 2 will be coupled with conjugate heat loss in the wall. This means that both sides at $x = 0$ in Fig. 1 share the same contact temperature

$$T_{\text{wall}}(x = 0^-) = T_{\text{flame}}(x = 0^+) \quad (18)$$

and the heat transfer

$$j_{q,\text{wall}}(x = 0^-) = T_{q,\text{flame}}(x = 0^+). \quad (19)$$

And the back-side of the wall is assumed to be fixed at 300 K. The wall is modeled to be stainless steel with a thickness of 2 mm, following the investigation on the influence of conjugate heat transfer for the side-wall quenching flame in Zirwes et al. (2021). All other material properties such as heat conductivity, heat capacity and density are also identical to those in Zirwes et al. (2021).

Figure 10 compares the quenching distances predicted by fixed wall temperature (solid symbol lines) and by considering conjugate heat loss in the wall (dashed symbol lines). We notice that there are almost no visible differences between both cases. In other words, the effect of considering the conjugate heat loss in the wall on the quenching distances is negligible. Near the quenching point, the wall temperature at $x = 0$ reaches its maximum value of around 310 K, which is an increase of about only 10 K. Consequently, the quenching distance is slightly changed within 0.5%. This can be attributed to fact that the time of the flame quenching is much shorter than the time-scale of the heat conductivity in the wall, so that the wall temperature has no sufficient time to react. Such conclusion is consistent with the observation in Zirwes et al. (2021), Häber and Suntz (2018) as well, where the methane-air flame quenching process is considered. However, it should be mentioned that the heat loss in the wall can affect the flame structures and quenching distances in other cases such as side-wall quenching configuration reported in Zhang et al. (2022) or

Fig. 10 Quenching distances versus fuel/air equivalence ratios for different hydrogen additions by considering fixed wall temperatures (solid symbol lines) and conjugate heat loss in the wall (dashed symbol lines)

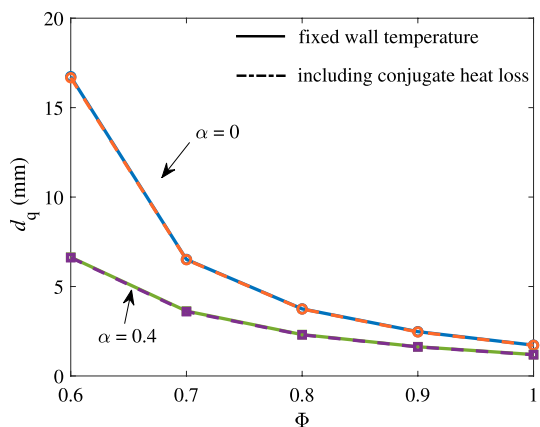
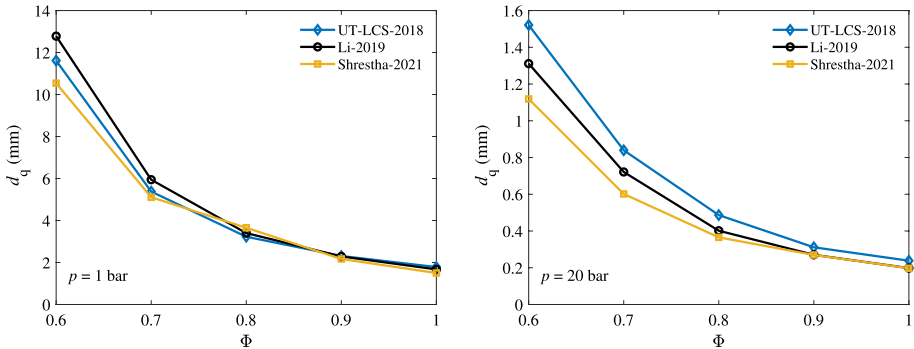


Table 2 Three different detailed chemical mechanisms and the corresponding numbers of involving species

Mechanism	Species no.	References
Li-2019	32	Li et al. (2019)
Shrestha-2021	30	Shrestha et al. (2021)
Otomo-2018 (UT-LCS)	31	Otomo et al. (2018)

**Fig. 11** Quenching distances d_q over fuel/air equivalence ratios Φ at two pressures for gas mixture with $\text{NH}_3:\text{H}_2 = 0.8:0.2$. Three different detailed chemical mechanisms are used, as listed in Table 2

turbulent flame-wall interaction reported in e.g. Zhao et al. (2018), Gruber et al. (2010) or use of other materials with lower heat conductivities (Kai et al. 2020).

5.3 Reaction Mechanisms

In this section, we focus on the influence of the chemical kinetics on the predicted quenching distance. Before performing the sensitivity analysis, it is interesting to investigate how large difference on the quenching distances exist, if different detailed chemistries are used. To show this, two more detailed chemical mechanisms, the Shrestha-2021 mechanism (Shrestha et al. 2021) and the Otomo-2018 (UT-LCS) mechanism (Otomo et al. 2018) (see Table 2), are used for the prediction of quenching distance for flame of gas mixture $\text{NH}_3:\text{H}_2 = 0.8:0.2$ with different fuel/air equivalence ratios at two pressures, as shown in Fig. 11. It is observed that the leaner the mixture is, the larger is the difference of predicted quenching distance for both pressures.

Note that there are also many other mechanisms such as Nakamura et al. (2017), Stagni et al. (2020) and Gotama et al. (2022). However, our aim here is only to state that there exist large differences using different chemical kinetics. Thus it is important to know which elementary reactions are especially important for the accuracy of the predicted quenching distance. If there are experiment measurements in the future, it is then recommended to test every chemical mechanism for its ability in the prediction of quenching distance. In order to answer this question, the sensitivity analysis is a helpful tool to quantify which elementary reactions are the key reactions.

The relative sensitivity $S^{\text{rel}}(d_q)$ used in this work describes the normalized sensitivity of d_q with respect to the reaction rate constant of one elementary reaction as:

$$\begin{aligned}
 S^{\text{rel}} &= \frac{k_r}{d_q} \cdot \frac{\partial d_q}{\partial k_r} \quad (\text{evaluated by finite difference}) \\
 &\approx \frac{k_r}{d_q} \cdot \frac{\Delta d_q}{\Delta k_r} = \frac{k_r}{d_q} \cdot \frac{d_q(2k_r) - d_q(k_r)}{2k_r - k_r} \\
 &= \frac{d_q(2k_r) - d_q(k_r)}{d_q(k_r)}.
 \end{aligned} \tag{20}$$

Figure 12 shows the sensitivity of the quenching distance $S^{\text{rel}}(d_q)$ (red bars) with respect to the reaction rate constants based on the Li-2019 mechanism (Li et al. 2019). Note that these values are shown in $-S^{\text{rel}}(d_q)$ for convenient readability. Together shown in this figure is the sensitivity of the laminar burning velocity $S^{\text{rel}}(\text{LBV})$ (blue bars), which is a common topic in other literature (c.f. da Rocha et al. 2019; Shrestha et al. 2021; Xiao et al. 2017). Several important observations can be addressed here:

- The $S^{\text{rel}}(d_q)$ has always an opposite sign of the $S^{\text{rel}}(\text{LBV})$. In other words, an increase of LBV leads to a decrease of d_q , and vice versa. This is because, as discussed above, that an increase of LBV means a higher heat release rate in the flame, and consequently more stable against quenching due to heat loss. Therefore, the d_q decreases with increasing LBVs.
- The LBV and the d_q are sensitive to the similar elementary reactions. Among them, the most sensitive elementary reaction is $\text{H} + \text{O}_2 = \text{OH} + \text{O}$. This indicates that an accurate prediction of LBV is prerequisite for an accurate prediction of d_q .

Fig. 12 sensitivity of both laminar burning velocity (blue bars) and the quenching distance (red bars) with respect to the reaction rates. Conditions: gas mixture with $\text{NH}_3:\text{H}_2 = 0.8:0.2$; fuel/air equivalent ratio $\Phi = 0.8$. $p = 1$ bar. Chemical mechanism (Li et al. 2019)

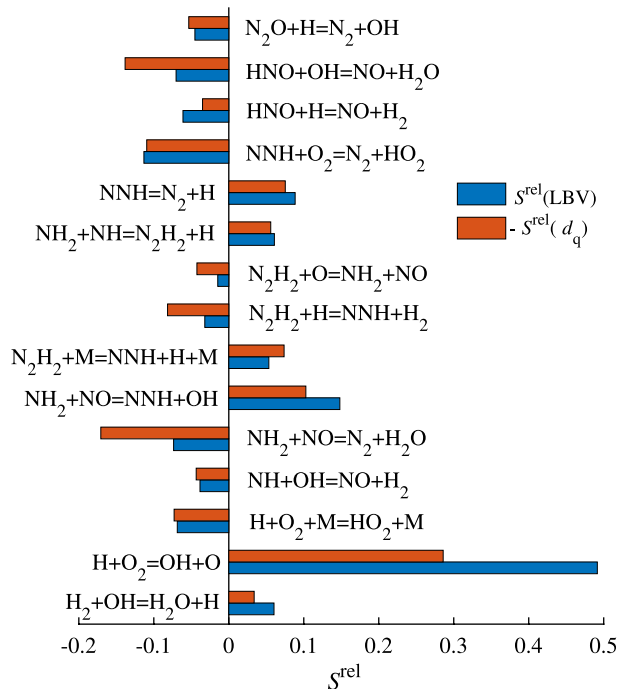
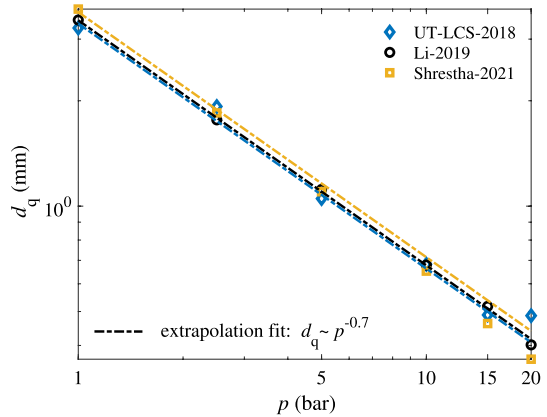


Fig. 13 Quenching distances versus pressure for gas mixture with 20% hydrogen addition ($\alpha = 0.2$) and fuel/air equivalence ratios $\Phi = 0.8$ for three detailed chemical kinetics listed in Table 2. Both axes in logarithmic scales



It should be mentioned that although this sensitivity analysis is based on the Li-2019 mechanism, these two observations also hold for the other two mechanisms considered (not shown here).

In Sect. 4.2 it is shown that the correlation between quenching distance d_q and pressure p follows a power function Eq. (14) by using the Li-2019 mechanism (Li et al. 2019). In Fig. 13 such correlation is also checked for other two mechanisms listed in Table 2. And it is observed that the power function of Eq. (14) is independent on the mechanisms we used.

6 Conclusions

The numerical investigation on the head-on quenching (HoQ) process of $\text{NH}_3\text{-H}_2\text{-air}$ flames is performed. The gas mixture is considered in the lean to stoichiometric range due to its practical application in gas turbines which operate under Dry Low NOx (DLN). Focusing on the quenching distance d_q , the main phenomenology findings of the present work are:

- The quenching distances decrease with increasing H_2 addition and increasing fuel/air equivalent ratios in range of lean to stoichiometric conditions for all pressures;
- The quenching distances decrease with increasing pressure, following the power function $d_q \sim p^{-0.7}$;
- An increasing quenching Peclet number Pe_q results in decreasing normalized wall heat loss φ , and an empirical extrapolation fit as a rational function has been suggested.

Furthermore, models and model parameters have been altered to study the sensitivity of the quenching distances. It is found that:

- The molecular transport model plays an important role, especially when the hydrogen contents are increased in the gas mixtures;
- The consideration of the conjugate heat loss in the wall during the quenching processes has negligible effect on the predicted quenching distance with a change of maximum 0.5% for the considered system;

- The predicted quenching distance is sensitive to several key elementary reactions such as $\text{H} + \text{O}_2 = \text{OH} + \text{H}$ and $\text{NH}_2 + \text{NO} = \text{N}_2 + \text{H}_2\text{O}$. And these key elementary reactions, which are significant for the accurate prediction of the quenching distances, are similar to those for the laminar burning velocity (LBV). This suggests that the accurate prediction of LBV is a prerequisite for an accurate prediction of quenching distance;
- although different detailed chemical mechanisms can provide different values of quenching distances, their dependence on pressure obeys the power function $d_q \sim p^{-0.7}$.

Acknowledgements Financial support from the German Research Foundation (DFG) - Grant Number 237267381 - TRR 150 is gratefully acknowledged. C. Chi would like to thank the DFG for its financial support within Project TH881/38-1 (DADOREN). S. Mashruk and A. Valera-Medina would appreciate the SAFE-AGT pilot (No. EP/T009314/1) with funding from the Engineering and Physical Sciences Research Council (EPSRC).

Author Contributions Conceptualization: CY; Methodology: CY, LC, CC and UM; Software and simulations: CY and UM; Validation: CY, CC and SM; Data analysis: CY, LC, CC, AVM; Writing-original draft preparation: CY and CC; Writing—review and editing: CY, LC, CC, SM, AVM and UM; Supervision: CY and UM; All authors have reviewed the manuscript.

Funding Open Access funding enabled and organized by Projekt DEAL. Funding was provided by Deutsche Forschungsgemeinschaft (Grant Nos. 237267381, TH881/38-1, 237267381). Engineering and Physical Sciences Research Council (Grant Nos. EP/T009314/1, EP/T009314/1).

Declarations

Conflict of interest The authors declare that they have no conflict of interest.

Open Access This article is licensed under a Creative Commons Attribution 4.0 International License, which permits use, sharing, adaptation, distribution and reproduction in any medium or format, as long as you give appropriate credit to the original author(s) and the source, provide a link to the Creative Commons licence, and indicate if changes were made. The images or other third party material in this article are included in the article's Creative Commons licence, unless indicated otherwise in a credit line to the material. If material is not included in the article's Creative Commons licence and your intended use is not permitted by statutory regulation or exceeds the permitted use, you will need to obtain permission directly from the copyright holder. To view a copy of this licence, visit <http://creativecommons.org/licenses/by/4.0/>.

References

- Andrae, J., Björnbohm, P., Edsberg, L.: Numerical studies of wall effects with laminar methane flames. *Combust. Flame* **128**(1–2), 165–180 (2002)
- Baigomohammadi, M., Roussel, O., Dion, C.M.: A numerical study of lean propane-air flame acceleration at the early stages of burning in cold and hot isothermal walled small-size tubes. *Flow Turbul. Combust.* **104**, 179–207 (2020)
- Bothe, D.: On the Maxwell-Stefan approach to multicomponent diffusion. In: Escher, J., et al. (eds.) *Parabolic Problems. Progress in Nonlinear Differential Equations and Their Applications*, vol. 80, pp. 81–93. Springer, Basel (2011)
- Boust, B., Sotton, J., Labuda, S., Bellenoue, M.: A thermal formulation for single-wall quenching of transient laminar flames. *Combust. Flame* **149**(3), 286–294 (2007)
- Bouvet, N., Halter, F., Chauveau, C., Yoon, Y.: On the effective Lewis number formulations for lean hydrogen/hydrocarbon/air mixtures. *Int. J. Hydrog. Energy* **38**(14), 5949–5960 (2013)
- Bruneaux, G., Akselvoll, K., Poinso, T., Ferziger, J.: Flame-wall interaction simulation in a turbulent channel flow. *Combust. Flame* **107**(1–2), 27–44 (1996)
- Bychkov, V., Liberman, M.A.: Dynamics and stability of premixed flames. *Phys. Rep.* **325**(4–5), 115–237 (2000)

- Chauvy, M., Delhom, B., Reveillon, J., Demoulin, F.-X.: Flame/wall interactions: laminar study of unburnt HC formation. *Flow Turbul. Combust.* **84**(3), 369–396 (2010)
- Chi, C., Han, W., Thévenin, D.: Effects of molecular diffusion modeling on turbulent premixed $\text{NH}_3/\text{H}_2/\text{air}$ flames. *Proc. Combust. Inst.* (2022)
- Chu, H., Ren, F., Xiang, L., Dong, S., Qiao, F., Xu, G.: Numerical investigation on combustion characteristics of laminar premixed n-heptane/air flames at elevated initial temperature and pressure. *J. Energy Inst.* **92**(6), 1821–1830 (2019)
- Colson, S., Hayakawa, A., Kudo, T., Kobayashi, H.: Extinction characteristics of ammonia/air counterflow premixed flames at various pressures. *J. Therm. Sci. Technol.* **11**(3), 48 (2016)
- Dabireau, F., Cuenot, B., Vermorel, O., Poinot, T.: Interaction of flames of $\text{H}_2 + \text{O}_2$ with inert walls. *Combust. Flame* **135**(1–2), 123–133 (2003)
- Dai, L., Gersen, S., Glarborg, P., Levinsky, H., Mokhov, A.: Experimental and numerical analysis of the autoignition behavior of NH_3 and NH_2/H_2 mixtures at high pressure. *Combust. Flame* **215**, 134–144 (2020)
- Daniel, W.: Flame quenching at the walls of an internal combustion engine. In: *Symposium (International) on Combustion*, vol. 6, pp. 886–894. Elsevier (1957)
- Ferguson, C.R., Keck, J.C.: On laminar flame quenching and its application to spark ignition engines. *Combust. Flame* **28**, 197–205 (1977)
- Ganter, S., Heinrich, A., Meier, T., Kuenne, G., Jainski, C., Ribmann, M.C., Dreizler, A., Janicka, J.: Numerical analysis of laminar methane-air side-wall-quenching. *Combust. Flame* **186**, 299–310 (2017)
- Gotama, G.J., Hayakawa, A., Okafor, E.C., Kanoshima, R., Hayashi, M., Kudo, T., Kobayashi, H.: Measurement of the laminar burning velocity and kinetics study of the importance of the hydrogen recovery mechanism of ammonia/hydrogen/air premixed flames. *Combust. Flame* **236**, 111753 (2022)
- Gruber, A., Sankaran, R., Hawkes, E.R., Chen, J.: Turbulent flame-wall interaction: a direct numerical simulation study. *J. Fluid Mech.* **658**, 5–32 (2010)
- Guiberti, T.F., Belhi, M., Damazo, J.S., Kwon, E., Roberts, W.L., Lacoste, D.A.: Quenching distance of laminar methane-air flames at cryogenic temperatures and implications for flame arrester design. *Appl. Energy Combust. Sci.* **1**, 100001 (2020)
- Guo, L., Zhai, M., Xu, S., Shen, Q., Dong, P., Bai, X.-S.: Flame characteristics of methane/air with hydrogen addition in the micro confined combustion space. *Int. J. Hydrog. Energy* **47**(44), 19319–19337 (2022)
- Häber, T., Suntz, R.: Effect of different wall materials and thermal-barrier coatings on the flame-wall interaction of laminar premixed methane and propane flames. *Int. J. Heat Fluid Flow* **69**, 95–105 (2018)
- He, X., Shu, B., Nascimento, D., Moshhammer, K., Costa, M., Fernandes, R.: Auto-ignition kinetics of ammonia and ammonia/hydrogen mixtures at intermediate temperatures and high pressures. *Combust. Flame* **206**, 189–200 (2019)
- Hirschfelder, J.O., Curtiss, C.F., Bird, R.B., Mayer, M.G.: *Molecular Theory of Gases and Liquids*, vol. 165. Wiley, New York (1964)
- Hou, D., Zhang, Z., Cheng, Q., Liu, B., Zhou, M., Li, G.: Experimental and kinetic studies of laminar burning velocities of ammonia with high Lewis number at elevated pressures. *Fuel* **320**, 123913 (2022)
- Ichikawa, A., Hayakawa, A., Kitagawa, Y., Somaratne, K.K.A., Kudo, T., Kobayashi, H.: Laminar burning velocity and Markstein length of ammonia/hydrogen/air premixed flames at elevated pressures. *Int. J. Hydrog. Energy* **40**(30), 9570–9578 (2015)
- Jing, Q., Huang, J., Liu, Q., Chen, X., Wang, Z., Liu, C.: The flame propagation characteristics and detonation parameters of ammonia/oxygen in a large-scale horizontal tube: As a carbon-free fuel and hydrogen-energy carrier. *Int. J. Hydrog. Energy* **46**(36), 19158–19170 (2021)
- Kaddar, D., Steinhäusen, M., Zirwes, T., Bockhorn, H., Hasse, C., Ferraro, F.: Combined effects of heat loss and curvature on turbulent flame-wall interaction in a premixed dimethyl ether/air flame. *Proc. Combust. Inst.* (2022)
- Kai, R., Masuda, R., Ikedo, T., Kurose, R.: Conjugate heat transfer analysis of methane/air premixed flame-wall interaction: a study on effect of wall material. *Appl. Therm. Eng.* **181**, 115947 (2020)
- Kee, R.J., Coltrin, M.E., Glarborg, P.: *Chemically Reacting Flow: Theory and Practice*. John Wiley & Sons, Hoboken (2005)
- Khateeb, A.A.: Stability limits and exhaust emissions from ammonia flames in a swirl combustor at elevated pressures. PhD thesis, King Abdullah University of Science and Technology (2020)
- Khateeb, A.A., Guiberti, T.F., Wang, G., Boyette, W.R., Younes, M., Jamal, A., Roberts, W.L.: Stability limits and no emissions of premixed swirl ammonia-air flames enriched with hydrogen or methane at elevated pressures. *Int. J. Hydrog. Energy* **46**(21), 11969–11981 (2021)

- Kosaka, H., Zentgraf, F., Scholtissek, A., Hasse, C., Dreizler, A.: Effect of flame-wall interaction on local heat release of methane and DME combustion in a side-wall quenching geometry. *Flow Turbul. Combust.* **104**, 1029–1046 (2020)
- Kovaleva, M., Gotama, G., Hayakawa, A., Okafor, E.C., Colson, S., Crayford, A., Kudo, T., Kobayashi, H.: The impact of Soret diffusion on the product gas characteristics of premixed ammonia/hydrogen/air flames stabilised in a stagnation flow. In: 14th Asia-Pacific Conference on Combustion (2023)
- Lai, J., Chakraborty, N.: Effects of Lewis number on head-on quenching of turbulent premixed flames: a direct numerical simulation analysis. *Flow Turbul. Combust.* **96**(2), 279–308 (2016)
- Lai, J., Wacks, D.H., Chakraborty, N.: Flow topology distribution in head-on quenching of turbulent premixed flame: a direct numerical simulation analysis. *Fuel* **224**, 186–209 (2018)
- Lapalme, D., Lemaire, R., Seers, P.: Assessment of the method for calculating the Lewis number of H₂/CO/CH₄ mixtures and comparison with experimental results. *Int. J. Hydrog. Energy* **42**(12), 8314–8328 (2017)
- Li, H.-M., Li, G.-X., Sun, Z.-Y., Zhai, Y., Zhou, Z.-H.: Research on cellular instabilities of lean premixed syngas flames under various hydrogen fractions using a constant volume vessel. *Energies* **7**(7), 4710–4726 (2014)
- Li, R., Konnov, A.A., He, G., Qin, F., Zhang, D.: Chemical mechanism development and reduction for combustion of NH₃/H₂/CH₄ mixtures. *Fuel* **257**, 116059 (2019)
- Li, J., Huang, H., Deng, L., He, Z., Osaka, Y., Kobayashi, N.: Effect of hydrogen addition on combustion and heat release characteristics of ammonia flame. *Energy* **175**, 604–617 (2019)
- Liang, W., Chen, Z., Yang, F., Zhang, H.: Effects of Soret diffusion on the laminar flame speed and Markstein length of syngas/air mixtures. *Proc. Combust. Inst.* **34**(1), 695–702 (2013)
- Maas, U., Warnatz, J.: Ignition processes in hydrogen-oxygen mixtures. *Combust. Flame* **74**(1), 53–69 (1988)
- Mari, R., Cuenot, B., Rocchi, J.-P., Selle, L., Duchaine, F.: Effect of pressure on hydrogen/oxygen coupled flame-wall interaction. *Combust. Flame* **168**, 409–419 (2016)
- Mashruk, S., Kovaleva, M., Alnasif, A., Chong, C.T., Hayakawa, A., Okafor, E.C., Valera-Medina, A.: Nitrogen oxide emissions analyses in ammonia/hydrogen/air premixed swirling flames. *Energy* **260**, 125183 (2022)
- Mei, B., Zhang, X., Ma, S., Cui, M., Guo, H., Cao, Z., Li, Y.: Experimental and kinetic modeling investigation on the laminar flame propagation of ammonia under oxygen enrichment and elevated pressure conditions. *Combust. Flame* **210**, 236–246 (2019)
- Nakamura, H., Hasegawa, S., Tezuka, T.: Kinetic modeling of ammonia/air weak flames in a micro flow reactor with a controlled temperature profile. *Combust. Flame* **185**, 16–27 (2017)
- Okafor, E.C., Tsukamoto, M., Hayakawa, A., Somaratne, K.K.A., Kudo, T., Tsujimura, T., Kobayashi, H.: Influence of wall heat loss on the emission characteristics of premixed ammonia-air swirling flames interacting with the combustor wall. *Proc. Combust. Inst.* **38**(4), 5139–5146 (2021)
- Otomo, J., Koshi, M., Mitsumori, T., Iwasaki, H., Yamada, K.: Chemical kinetic modeling of ammonia oxidation with improved reaction mechanism for ammonia/air and ammonia/hydrogen/air combustion. *Int. J. Hydrog. Energy* **43**(5), 3004–3014 (2018)
- Owston, R., Magi, V., Abraham, J.: Interactions of hydrogen flames with walls: influence of wall temperature, pressure, equivalence ratio, and diluents. *Int. J. Hydrog. Energy* **32**(12), 2094–2104 (2007)
- Palullli, R., Talei, M., Gordon, R.L.: Unsteady flame-wall interaction: impact on co emission and wall heat flux. *Combust. Flame* **207**, 406–416 (2019)
- Poinsot, T., Veynante, D.: *Theoretical and Numerical Combustion*. RT Edwards, Inc., South Lanarkshire (2005)
- Poinsot, T., Haworth, D.C., Bruneaux, G.: Direct simulation and modeling of flame-wall interaction for premixed turbulent combustion. *Combust. Flame* **95**(1–2), 118–132 (1993)
- Popp, P., Smooke, M., Baum, M.: Heterogeneous/homogeneous reaction and transport coupling during flame-wall interaction. In: *Symposium (International) on Combustion*, vol. 26, pp. 2693–2700. Elsevier (1996)
- Popp, P., Baum, M.: Analysis of wall heat fluxes, reaction mechanisms, and unburnt hydrocarbons during the head-on quenching of a laminar methane flame. *Combust. Flame* **108**(3), 327–348 (1997)
- Potter, A., Jr.: Flame quenching. In: *Progress in Combustion Science and Technology*, pp. 145–181. Elsevier, Amsterdam (1960)
- Rißmann, M., Jainski, C., Mann, M., Dreizler, A.: Flame-flow interaction in premixed turbulent flames during transient head-on quenching. *Flow Turbul. Combust.* **98**(4), 1025–1038 (2017)
- Rocha, R.C., Costa, M., Bai, X.-S.: Chemical kinetic modelling of ammonia/hydrogen/air ignition, premixed flame propagation and no emission. *Fuel* **246**, 24–33 (2019)

- Salimath, P.S., Ertesvåg, I.S., Gruber, A.: Computational analysis of premixed methane-air flame interacting with a solid wall or a hydrogen porous wall. *Fuel* **272**, 117658 (2020)
- Savard, B., Blanquart, G.: An a priori model for the effective species Lewis numbers in premixed turbulent flames. *Combust. Flame* **161**(6), 1547–1557 (2014)
- Shrestha, K.P., Lhuillier, C., Barbosa, A.A., Brequigny, P., Contino, F., Mounaïm-Rousselle, C., Seidel, L., Mauss, F.: An experimental and modeling study of ammonia with enriched oxygen content and ammonia/hydrogen laminar flame speed at elevated pressure and temperature. *Proc. Combust. Inst.* **38**(2), 2163–2174 (2021)
- Stagni, A., Cavallotti, C., Arunthanayothin, S., Song, Y., Herbinet, O., Battin-Leclerc, F., Faravelli, T.: An experimental, theoretical and kinetic-modeling study of the gas-phase oxidation of ammonia. *React. Chem. Eng.* **5**(4), 696–711 (2020)
- Strassacker, C., Bykov, V., Maas, U.: Redim reduced modeling of quenching at a cold wall including heterogeneous wall reactions. *Int. J. Heat Fluid Flow* **69**, 185–193 (2018)
- Strassacker, C., Bykov, V., Maas, U.: Redim reduced modeling of flame quenching at a cold wall—the influence of detailed transport models and detailed mechanisms. *Combust. Sci. Technol.* **191**(2), 208–222 (2019)
- Strassacker, C., Bykov, V., Maas, U.: Reduced modeling of flame-wall-interactions of premixed iso-octane-air systems including detailed transport and surface reactions. *Proc. Combust. Inst.* **38**(1), 1063–1070 (2021)
- Suckart, D., Linse, D., Schutting, E., Eichlleder, H.: Experimental and simulative investigation of flame-wall interactions and quenching in spark-ignition engines. *Automot. Engine Technol.* **2**(1), 25–38 (2017)
- Valera-Medina, A., Xiao, H., Owen-Jones, M., David, W.I., Bowen, P.: Ammonia for power. *Prog. Energy Combust. Sci.* **69**, 63–102 (2018)
- Valera-Medina, A., Amer-Hatem, F., Azad, A., Dedoussi, I., De Joannon, M., Fernandes, R., Glarborg, P., Hashemi, H., He, X., Mashruk, S.: Review on ammonia as a potential fuel: from synthesis to economics. *Energy Fuels* **35**(9), 6964–7029 (2021)
- Vosen, S., Greif, R., Westbrook, C.: Unsteady heat transfer during laminar flame quenching. In: *Symposium (International) on Combustion*, 20, pp. 75–83. Elsevier (1985)
- Wan, S., Fan, Y., Maruta, K., Suzuki, Y.: Wall chemical effect of metal surfaces on DME/air cool flame in a micro flow reactor. *Proc. Combust. Inst.* **37**(4), 5655–5662 (2019)
- Wang, D., Ji, C., Wang, S., Yang, J., Wang, Z.: Numerical study of the premixed ammonia–hydrogen combustion under engine-relevant conditions. *Int. J. Hydrog. Energy* **46**(2), 2667–2683 (2021)
- Wei, X., Zhang, M., An, Z., Wang, J., Huang, Z., Tan, H.: Large eddy simulation on flame topologies and the blow-off characteristics of ammonia/air flame in a model gas turbine combustor. *Fuel* **298**, 120846 (2021)
- Westbrook, C.K., Adamczyk, A.A., Lavoie, G.A.: A numerical study of laminar flame wall quenching. *Combust. Flame* **40**, 81–99 (1981)
- Xiao, H., Valera-Medina, A., Bowen, P.J.: Modeling combustion of ammonia/hydrogen fuel blends under gas turbine conditions. *Energy Fuels* **31**(8), 8631–8642 (2017)
- Yenerdag, B., Minamoto, Y., Aoki, K., Shimura, M., Nada, Y., Tanahashi, M.: Flame-wall interactions of lean premixed flames under elevated, rising pressure conditions. *Fuel* **189**, 8–14 (2017)
- Yu, C., Böhlke, T., Valera-Medina, A., Yang, B., Maas, U.: Flame-solid interaction: thermomechanical analysis for a steady laminar stagnation flow stoichiometric $\text{NH}_3\text{-H}_2$ flame at a plane wall. *Energy Fuels* **37**(4), 3294–3306 (2023)
- Zhang, F., Zirwes, T., Häber, T., Bockhorn, H., Trimis, D., Suntz, R., Stapf, D.: Correlation of heat loss with quenching distance during transient flame-wall interaction. *Proc. Combust. Inst.* (2022)
- Zhang, J., Mei, B., Li, W., Fang, J., Zhang, Y., Cao, C., Li, Y.: Unraveling pressure effects in laminar flame propagation of ammonia: a comparative study with hydrogen, methane, and ammonia/hydrogen. *Energy Fuels* **36**(15), 8528–8537 (2022)
- Zhao, P., Wang, L., Chakraborty, N.: Analysis of the flame-wall interaction in premixed turbulent combustion. *J. Fluid Mech.* **848**, 193–218 (2018)
- Zirwes, T., Häber, T., Zhang, F., Kosaka, H., Dreizler, A., Steinhausen, M., Hasse, C., Stagni, A., Trimis, D., Suntz, R.: Numerical study of quenching distances for side-wall quenching using detailed diffusion and chemistry. *Flow Turbul. Combust.* **106**(2), 649–679 (2021)